JOURNAL OF MATERIALS SCIENCE 31 (1996) 1625–1631

Effect of second phase precipitates on recovery and recrystallization behaviour of cold-worked Al2024–SiC_p composites

R. MANNA, J. SARKAR, M.K. SURAPPA
Centre For Advanced Study, Department of Metallurgy, Indian Institute of Science, Bangalore 560 012, India

The restoration behaviour of SiC particle reinforced 2024-aluminium composite has been studied under conditions where recrystallization–grain growth and precipitation occur concurrently. An emphasis has been given to understanding the recrystallization–precipitation interaction, in the presence of SiC_p, during annealing. The composite was fabricated by a casting route followed by hot extrusion. Samples were cold deformed to a reduction in height of either 30 or 42 per cent following a heat treatment. The kinetics of recrystallization has been studied in the temperature range 100–485 °C. Recrystallization has been monitored by optical microscopy, coupled with hardness measurements. It has been observed that the composite has a lower recrystallization temperature compared to that of an unreinforced alloy under identical annealing conditions. Following recrystallization, grain growth has been noticed in the composite. Although the degree of cold deformation showed some effect on the recrystallization temperature of the composite, it was found to be a weak controlling factor for average recrystallized grain size. Results showed that, in spite of the hardness reduction due to recrystallization–grain growth, the hardness of a composite can be partially restored by concurrent solid solution hardening (dissolution of precipitates) and also by the generation of dislocations during quenching to a low temperature.

1. Introduction

The presence of second phase particles in aluminium alloys can be of particular significance for the modification of alloy recrystallization and grain growth behaviour [1–8]. They can directly affect various aspects of recrystallization, such as the kinetics and the grain size and therefore play an important role in the thermomechanical processing of metal matrix composites (MMCs). This is thought to be an indirect result of dislocations and internal stresses generated on cooling by differential thermal contraction between the particles and matrix alloy [9, 10]. For ceramic particles of the size range encountered in MMCs, the plastic relaxation results in a region close to the particle being rotated with respect to the matrix, and such a region is often called a "deformation zone" [11]. Particles of diameter greater than about 1.0 μm may stimulate the nucleation of recrystallized grains in the deformation zone adjacent to the particles [12]. This is often known as particle stimulated nucleation (PSN). Systems containing both large and fine particles may show accelerated or retarded recrystallization kinetics depending on the (F_v/d) ratio [12], where d is the average size of the particles and F_v is the volume fraction of the ceramic particles. The results of a large number of investigations show that recrystallization is impeded when $F_v/d \geqslant 0.1\ \mu m^{-1}$ [12]. If the particles are closely spaced then the subgrain growth necessary for the nucleation is impeded and, on annealing the material recovers but does not recrystallize [12]. Since the precipitation or dissolution of second phases and recrystallization of the cold deformed material can take place concurrently in many age hardenable aluminium alloy based MMCs, the final microstructure will be controlled either by: (i) the accelerated recrystallization due to large particles or by (ii) the Zener pinning [13] of grain boundaries by fine precipitates. Thus, there is a need to understand the effect that concurrent precipitation or dissolution of second phases has on recrystallization and grain growth in MMCs [14, 15].

The present study, therefore, involves a preliminary investigation aimed at understanding the effect of large reinforcement as well as concurrent dissolution of precipitates on recrystallization and grain growth in 5 vol% SiC particle reinforced Al2024 matrix composite materials.

2. Experimental procedures

An Al2024–SiC particle (SiC_p) reinforced MMC was fabricated by a casting route [16]. An extra amount (1 wt%) of commercially pure Mg was added to the melt in order to increase the wettability between the

0022–2461

TABLE I Chemical composition of the alloy (wt%) used for the present study

Cu	Mg	Mn	Si	Trace	Al
3.67	2.30	<0.08	0.45	<0.16	Balance

reinforcement and the matrix alloy. The final composition of the alloy used in the composites as well as in an unreinforced reference material is given in Table I. In order to facilitate the microstructural studies, the SiC_p concentration was chosen to be as low as 5 vol%. SiC_p of average size 12 μm and aspect ratio 1:1 to 5:1 were used as reinforcement. Subsequently, as-cast billets of both composite and unreinforced alloy were hot extruded (extrusion ratio = 18:1) at a temperature of 485 °C. Cylindrical specimens (15 mm in height and 10 mm diameter) of these materials were solution treated at 485 °C for 1.5 h and then slowly cooled to room temperature (25 °C) in order to obtain precipitates, such as Al–Cu, Al–Cu–Mg etc, before being subjected to cold deformation. Immediately, specimens were subjected to uniaxial compression, using a servo-hydraulic testing machine (Instron 8032), at room temperature in a direction parallel to the extrusion direction with a ram speed of 0.01 mm s^{-1}. Specimens of composites were cold deformed at two levels i.e. 30% and 42% reduction in height. The unreinforced alloy specimens were subjected only to a 30% reduction in height. Cold worked samples were initially isochronally annealed (one hour) in the temperature range 100–485 °C in an air furnace in order to determine the recrystallization temperature. The samples were also subjected to isothermal annealing at two different temperatures for several intervals of time, up to 10^5 s, in order to study the recrystallization kinetics. Following annealing, all the samples were water-quenched to room temperature and subsequently hardness measurements (Vickers at 5 kgf load) were done on the polished surface perpendicular to compression axis. On an average, ten hardness measurements were performed on each specimen and the average value will be reported in the following sections. The grain size measurements were carried out using the linear intercept method [17].

3. Results and discussion

The initial microstructure of the composite i.e., prior to cold deformation at room temperature is shown in Fig. 1. The microstructure contains equiaxed grains of average size 72.3 μm and precipitates of size 1.5–5 μm. The volume percent of precipitates was found to be 4.7. Fig. 2 shows the hardness variation as a function of the percentage of cold deformation at room temperature. The curve reveals that the hardness increases monotonically from 80 VPN at zero reduction to 132 VPN at 42% cold reduction. The hardness of the 30% cold deformed MMC is about 128 VPN. Although, there is not much difference in hardness between 30% and 42% cold deformed MMC, isochronal and isothermal treatments were carried out in order to understand the material behaviour and its trend under slightly varying cold reduction.

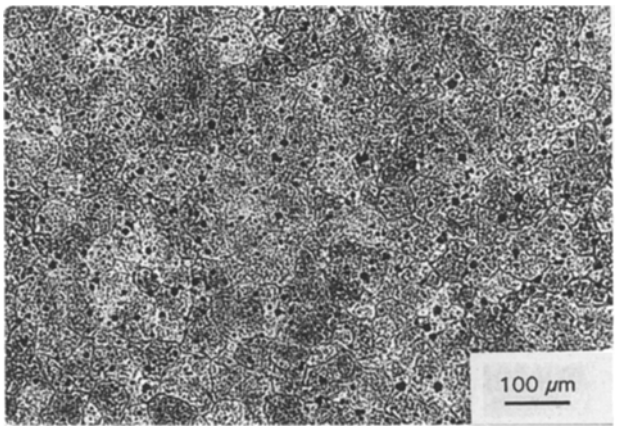

Figure 1 Optical micrograph of MMC prior to cold deformation.

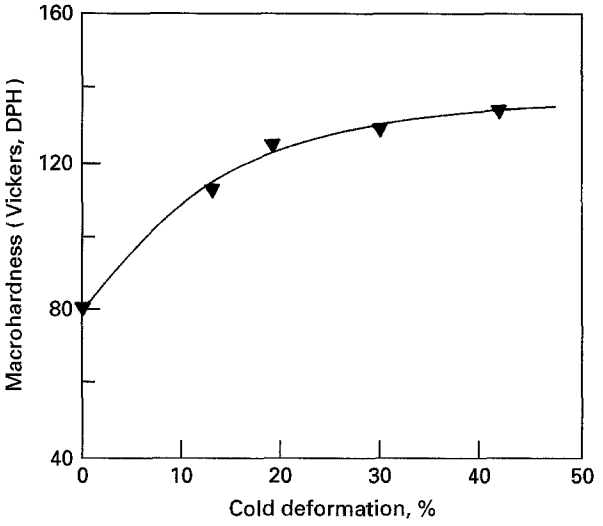

Figure 2 Hardness variation as a function of percentage of cold deformation.

3.1. Isochronal annealing for one hour

Fig. 3 shows the isochronal annealing plots (hardness versus temperature) for both 30% and 42% cold deformation MMCs. There is a steep drop in hardness above 200 °C in both the MMCs, but the minimum hardness values are different and these troughs occur at different temperatures. In the 30% cold deformed MMC the minimum occurs at 375 °C, whereas for the 42% cold deformed MMC the minimum occurs at 350 °C. Evidently, an increase in cold reduction by 12% decreases the temperature that corresponds to minimum hardness by 25 °C when all other parameters are same. Moreover, the hardness drop is greater in the case of the 42% cold deformed MMC, by 8 VPN, than that of the 30% cold deformed MMC. It should be noted that the hardness corresponding to minima are well below the hardness of the MMC at zero cold reduction (80 VPN). The grain size measurements (Table II) show that there is no grain refinement below 300 °C but that the hardness drops steadily. This indicates the occurrence of recovery below this temperature. Possibly, the movement of dislocations

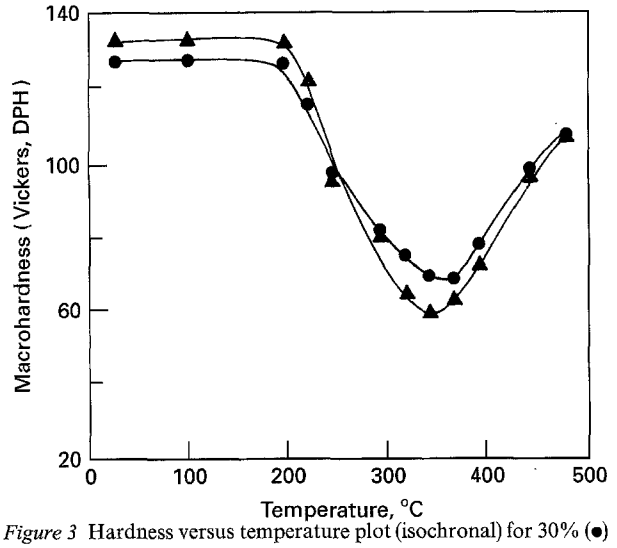

Figure 3 Hardness versus temperature plot (isochronal) for 30% (●) and 42% (▲) cold deformed MMCs.

TABLE II Grain size variation with temperature in MMCs

Temperature (°C)	Average grain size (μm)
42% cold deformed MMC	
$T \leqslant 300$	76.3
$380 \leqslant T \leqslant 400$	22.4
$T \approx 485$	32.8
30% cold deformed MMC	
$T \leqslant 300$	72.3
$T \approx 400$	24.2
$T \approx 485$	32.0

and cell-walls are restricted due to the presence of fine precipitates (Zener-pinning [13]), such as $CuAl_2$ (θ phase), $AlCu_2Mg$ (*S* phase) etc [18]. Consequently, recrystallization is prevented and only recovery has taken place. As the annealing temperature is increased the precipitates become relatively coarser and thus cease to behave as an effective barrier to the movement of dislocations, thereby allowing recrystallization to take place. Thus at temperatures above 300 °C the increased mobility allows low angle grain boundaries and subgrain boundaries to easily move to adjacent high angle boundaries thereby promoting recrystallization. Fig. 4 shows the microstructure containing equiaxed recrystallized grains (average size 24.2 μm) in 30% cold deformed MMC after isochronal annealing at 400 °C. However, the size of the recrystallized grains are much smaller near the SiC_p clusters. Similar observation has been made by Shahani and Clyne [6].

In both the MMCs the hardness values again increase with increasing temperature above a temperature which corresponds to minimum hardness. In the 42% cold deformed MMC the hardness increases from the minimum (60 VPN) at 350 °C to a hardness level of 108 VPN at 485 °C. Similarly, in the 30% cold deformed MMC the hardness increases from 68 VPN to 108 VPN at 485 °C with an increase in temperature above 375 °C. Fig. 5 shows the microstructure of the 30% cold deformed MMC annealed at 485 °C for one hour. The microstructure clearly reveals that appreciable amounts of grain growth has taken place in this material.

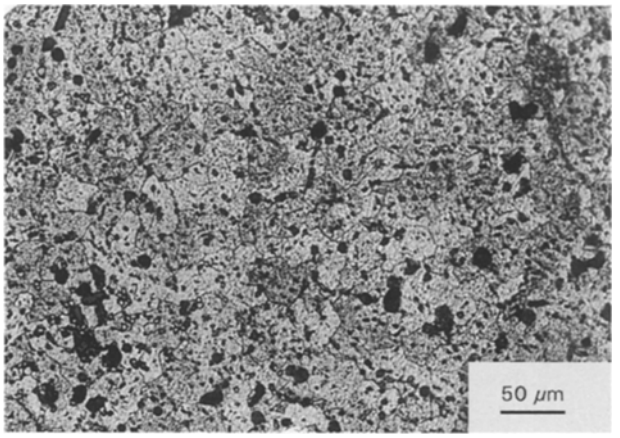

Figure 4 Optical micrograph of 30% cold deformed MMC annealed at 400 °C for one hour.

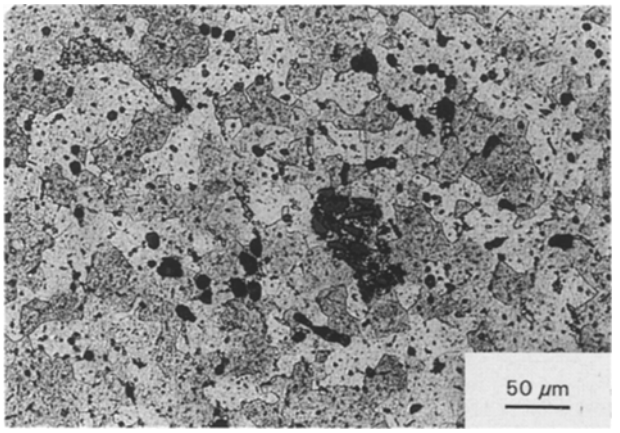

Figure 5 Optical micrograph of 30% cold deformed MMC annealed at 485 °C for one hour.

The increase in hardness is caused primarily because of solid solution hardening created by the dissolution of the θ phase which is present in the matrix after annealing at 485 °C, before it is subjected to cold deformation. Apart from the θ phase some other types of precipitates are present in the matrix, but the θ phase has the low dissolution temperature of 375 °C [18]. A second contributing factor is the generation of dislocations near SiC_p created by differential thermal contraction between the SiC_p and matrix alloy on quenching [9].

For comparison purposes a 30% cold deformed unreinforced alloy has been taken as a reference material. Table III lists the approximate recrystallization temperatures and average grain sizes for both unreinforced alloy and composite revealed in the isochronal annealing studies. It is clear from the isochronal plot for the 30% cold deformed unreinforced alloy (Fig. 6) that MMCs show a similar trend to that of the unreinforced alloy. There exists a steep decrease in hardness above 200 °C to a minimum at about 350 °C, followed by an increase in hardness with increasing temperature. In the case of the unreinforced alloy a drop in hardness of 41.1 VPN is observed up to the minimum which is smaller than that of the 30% cold deformed MMC (60 VPN). In the unreinforced alloy, there is no

TABLE III Recrystallization temperatures (Rex. temp.) and average grain sizes for cold deformed (C. D.) unreinforced alloy and MMCs

Material	Rex. temp. (°C)	Average grain size (μm)
30% C. D. unreinforced alloy	≈ 425	30.6
30% C. D. MMC	≈ 400	24.2
42% C. D. MMC	≈ 380	22.4

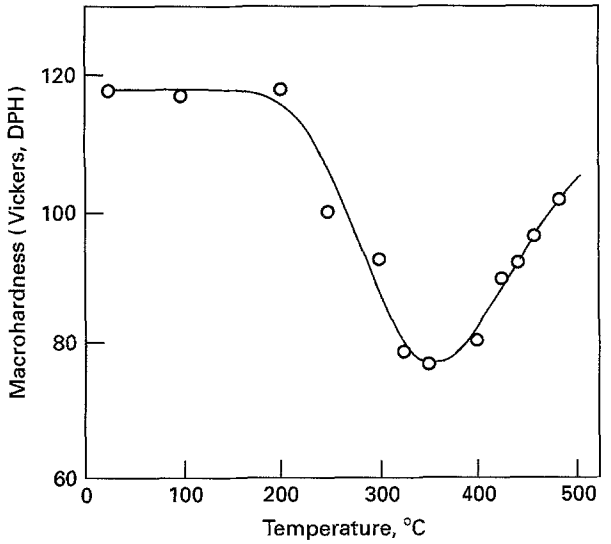

Figure 6 Hardness versus temperature plot (isochronal) for 30% cold deformed unreinforced alloy.

significant decrease in the average grain size up to a temperature of 300 °C, but beyond 400 °C considerable grain refinement is noted. The average grain size of the initial material (74.0 μm) reduces to less than half (30.6 μm) after recrystallization. The increase in hardness after the trough is much smaller in the case of the unreinforced alloy (24.4 VPN) compared to 30% cold deformed MMC (40 VPN). This is attributed to the absence of a hardness contribution from differential thermal contraction [9] in the case of the unreinforced alloy.

After recrystallization, grain growth has been observed in both the MMCs and also in the unreinforced alloy, but to different extents as is shown in Table IV. The solid solution hardening continues concurrently with grain growth with increasing temperature. Although, the hardness should drop because of the grain growth in MMCs, the contribution due to solid solution hardening and also hardening due to the generation of dislocations caused by differential thermal contraction between SiC_p and the matrix alloy during quenching are sufficient not only to compensate the hardness drop but also to increase it further. In summary, the shape of the isochronal curves is determined by three phenomena; (i) the recrystallization and grain growth, (ii) the solid solution hardening due to dissolution of precipitates and (iii) the hardness increase due to the generation of dislocations caused by differential thermal contraction between SiC_p and the matrix alloy during quenching.

TABLE IV Grain size variation during isothermal annealing of cold deformed (C. D.) MMCs and unreinforced alloy at 485 °C

Material	Time (s)	Average grain size (μm)
42% C. D. MMC	10.0	74.3
	150.0	22.5
	100 000.0	40.0
30% C. D. MMC	10.0	70.0
	200.0	24.9
	100 000.0	36.9
30% C.D. unreinforced alloy	10.0	74.0
	300.0	30.6
	100 000.0	53.0

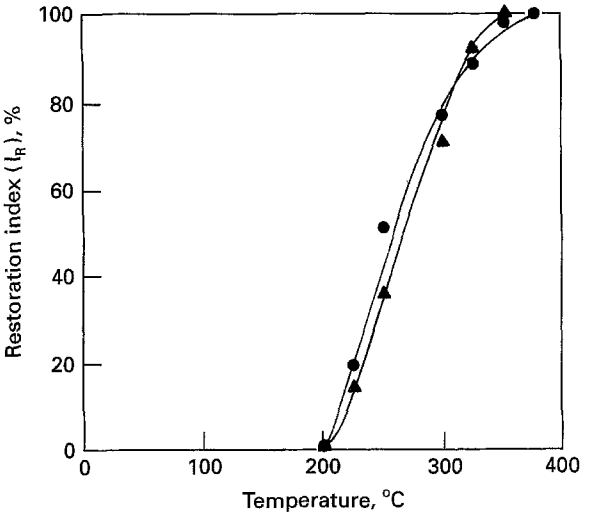

Figure 7 Restoration index (I_r) versus temperature plot for 30% (●) and 42% (▲) cold deformed MMCs.

3.1.1. Restoration index

The variation of hardness with temperature can be expressed in terms of a restoration index (I_r), which is given by the expression [15]:

$$I_r = (H_o - H_i) \times 100/(H_o - H_r) \quad (1)$$

where H_o is the hardness of the as-deformed material, H_i is the hardness measured immediately after annealing at a particular temperature and H_r is the minimum hardness obtained from an isochronal plot. Fig. 7 shows the variation of the restoration index with annealing temperature for the 30% and 42% cold deformed MMCs. It is clear that the hardness drop is prominent only above 200 °C and that the trend in the drop in hardness is the same in both cases. However, above 325 °C, i.e., in the recrystallization range, the restoration index of the 42% cold deformed MMC is greater than that of the 30% cold deformed MMC. This indicates that enhanced cold deformation accelerates the recrystallization process. This has also been confirmed by the recrystallization temperature of the composites listed in Table III.

3.2. Isothermal annealing

Isothermal annealing curves (hardness versus annealing time) have been plotted in order to study the

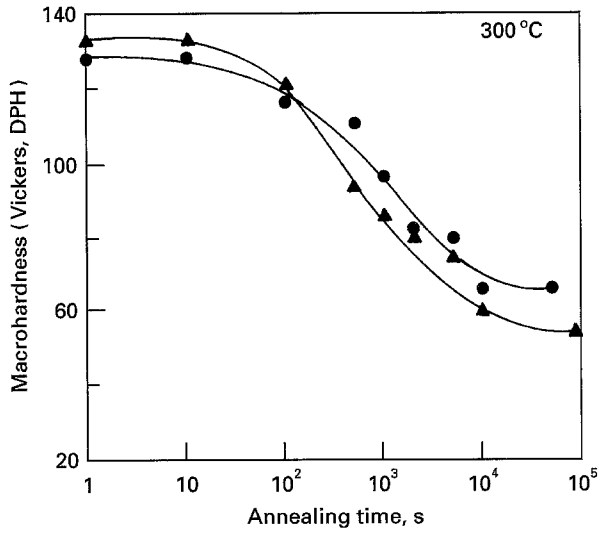

Figure 8 Hardness versus time plot (isothermal) for 30% (•) and 42% (▲) cold deformed MMCs at 300 °C.

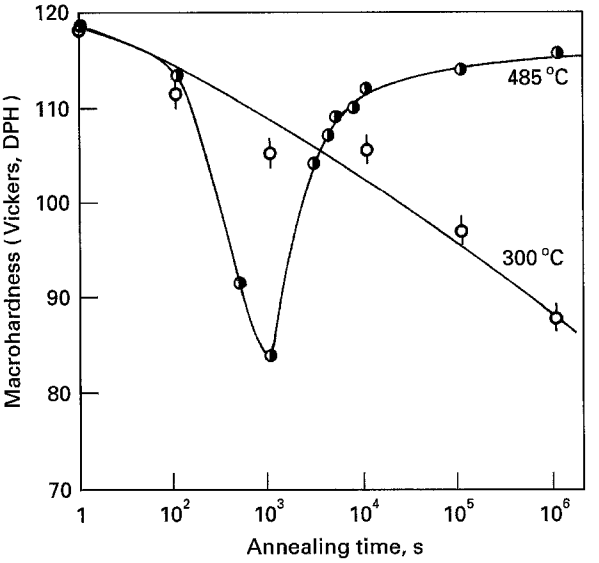

Figure 9 Hardness versus time plot (isothermal) for 30% cold deformed unreinforced alloy at 300 °C (♀) and 485 °C (◑).

kinetics of recrystallization and grain growth in MMCs and also in the unreinforced alloy. Fig. 8 shows the isothermal plots for the MMCs at 300 °C. As has been stated earlier, the recrystallization temperatures of MMCs are above 375 °C and consequently recrystallization is not responsible for the hardness drop in this case. It is tentatively expected that the coarsening of precipitates may cause softening of the MMCs. Moreover, grain size measurements confirm that there is no grain refinement with increasing time. Thus the drop in hardness is attributed to a combined effect of the coarsening of precipitates and also the recovery of the matrix. The trend of the isothermal curves is identical for both the 30% and 42% cold deformed MMCs.

Similarly, isothermal plots (Fig. 9) have been plotted for the 30% cold deformed unreinforced alloy. The trend in the isothermal annealing plot for MMCs at 300 °C is found to be similar to that of the unreinforced alloy under identical annealing conditions. A comparison shows that the hardness drop in MMC after 10^5 s is about two times that of the unreinforced alloy. The coarsening of precipitates and also the slow recovery of matrix in the absence of SiC_p seem to cause less softening in the unreinforced alloy. The grain size measurements reveal that there is no grain refinement.

Isothermal plots, (Fig. 10), have also been produced for MMCs at 485 °C which is higher than the recrystallization temperature. This temperature is high enough to promote restoration processes (recrystallization–grain growth) and consequently the hardness drops rapidly within 50–60 s and again increases with increasing annealing time. Within the first 50–60 s, the hardness drops by 47 VPN and 41 VPN in the 42% and 30% cold deformed MMCs, respectively. Fig. 11(a) shows the microstructure of the 42% cold deformed MMC annealed at 485 °C for 150 s. The microstructure contains fine equiaxed recrystallized grains of average size 22.5 μm. Fig. 11(b) shows the microstructure of the 42% cold deformed MMC annealed at 485 °C for 10^5 s. Unlike the previous sample,

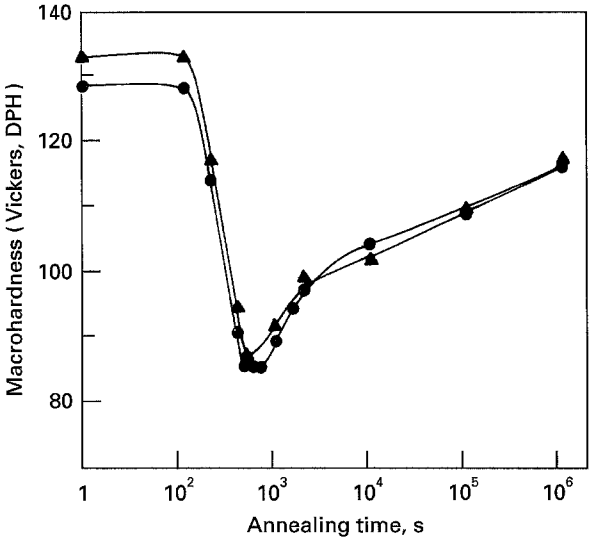

Figure 10 Hardness versus time plot (isothermal) for 30% (•) and 42% (▲) cold deformed MMCs at 485 °C.

the microstructure contains coarse equiaxed grains of average size 40 μm. From Fig. 12 it is obvious that considerable grain refinement has taken place at about 150 s in the 42% cold deformed MMC and at 200 s in the 30% cold deformed MMC, and that these are the times required for the complete recrystallization.

However, beyond these times the hardness of the recrystallized MMCs again increases monotonically. It should be noted that the minimum hardness values in both the MMCs are a little higher than the hardness of the initial material (80 VPN) prior to cold deformation. It should be noted that at 485 °C both the *S* phase and the θ phase are dissolving into the alloy [18]. The dissolution of increasing amounts of the second phases with time enhances the contribution of solid solution hardening over softening mechanisms such as grain growth to the extent that after 10^5 s, the hardness of both the MMCs reach a value of 116 VPN.

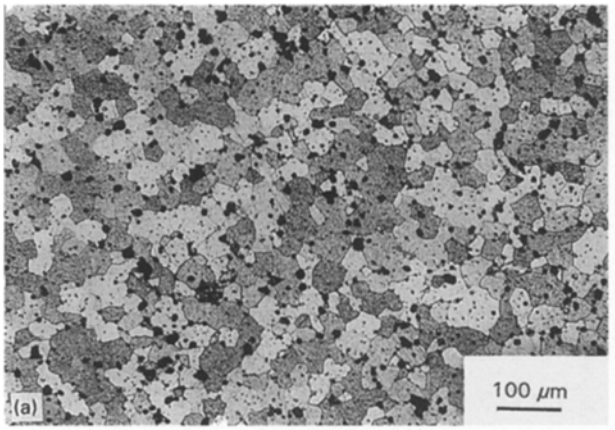

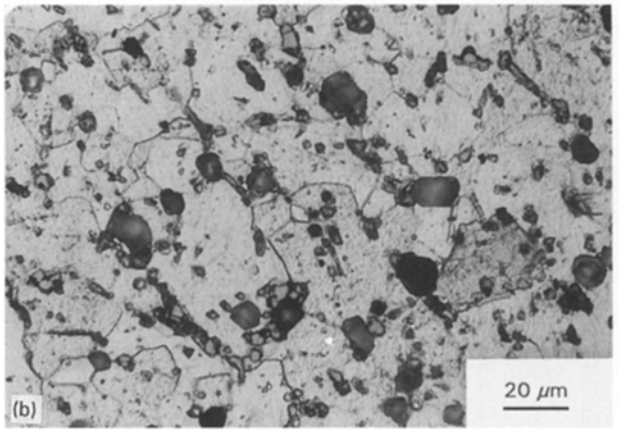

Figure 11 Optical micrographs of 42% cold deformed MMC annealed at 485 °C for (a) 150 s and (b) 10^5 s, respectively.

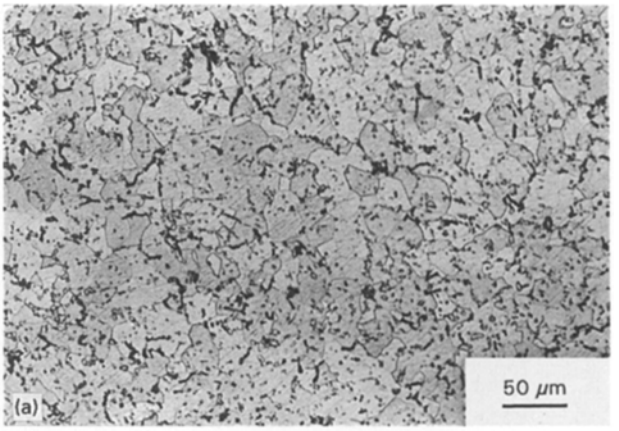

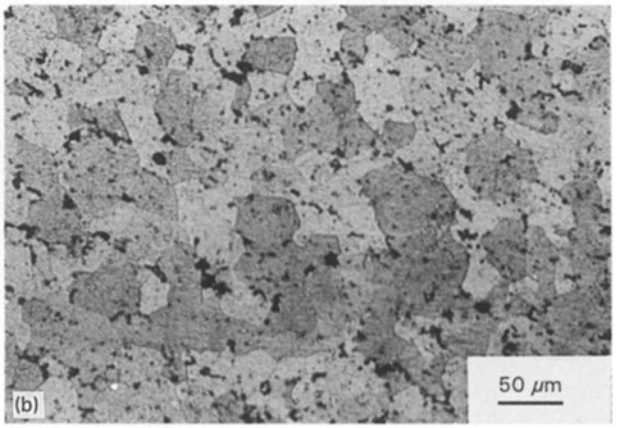

Figure 13 Optical micrographs of 30% cold deformed unreinforced alloy annealed at 485 °C for (a) 300 s and (b) 10^5 s, respectively.

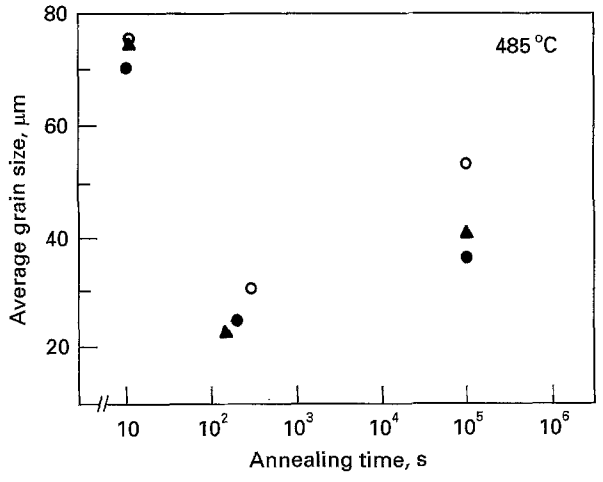

Figure 12 Average grain size variation in: 42% cold deformed MMC (▲), 30% cold deformed MMC (●) and 30% cold deformed unreinforced alloy (○) with time.

The isothermal plot at 450 °C for the 30% cold deformed unreinforced alloy (Fig. 9) shows that the initial hardness drops by 34 VPN within an interval of 100 s and then increases by a maximum of 31 VPN with increasing time. The reason for this behaviour seems to be the same as that in the case of the 30% cold deformed MMC. Fig. 13(a) shows the microstructure of the 30% cold deformed unreinforced alloy annealed at 485 °C for 300 s. The microstructure contains fine equiaxed recrystallized grains along with precipitates. However, as is shown in (Fig. 13(b)) the microstructure after annealing for 10^5 s shows the occurrence of an appreciable amount of grain growth. Table IV reveals that recrystallization is completed after an interval of 300 s which results in a minimum grain size of 30.6 μm. The minimum hardness in this case is much higher than that of the 30% cold deformed MMC.

The overall trend shows that the kinetics of recrystallization are faster in the MMCs compared to the unreinforced alloy. This is thought to be due to the difference between the substructures that develop during cold deformation in MMCs and in the unreinforced alloy. In the unreinforced alloy the distribution of strain is more uniform in comparison to MMCs. This is because of the non-uniform plastic deformation of the two phases in MMCs i.e. soft alloy matrix and non-deformable SiC particles. It results in a "deformation zone" [11] which in turn creates a steep strain gradient in the vicinity of particles in the MMCs. The parameters that contribute to promote faster recrystallization in MMCs than in the case of unreinforced alloy include;

(i) The lattice rotation associated with the subgrains in the deformation zone is closer to the reinforcements [19].
(ii) Stored energy in the deformation zone provides an additional driving force for the recrystallization.

Thus deformation zones provide preferential sites for nucleation during annealing, but they are absent in the case of unreinforced alloy. These arguments are consistent with the observations made in similar studies to ours which demonstrated that the presence of large reinforcements accelerate recrystallization in aluminium alloys [6].

4. Conclusions

The present investigations have led to the following conclusions:

1. The recrystallization temperature of an MMC is sensitive to the percentage of cold deformation as is observed in many monolithic materials. The MMCs show a lower recrystallization temperature compared to that of the unreinforced alloy under identical annealing conditions. In the MMCs large SiC particles act as nucleation sites and stimulate the recrystallization kinetics.
2. The average size of recrystallized grains in a MMC is found to be a weak function of the percentage of cold deformation.
3. Although recrystallization is a softening phenomena that occurs during annealing, the hardness of the MMCs can be partly restored by solid solution hardening due to the concurrent dissolution of precipitates at elevated temperature.
4. Grain growth has been observed in MMCs following recrystallization. Similar to recrystallization, hardness increases due to solid solution hardening even during grain growth in these composites.

5. Appendix

This study suggests many additional experiments that could be performed to elucidate the precipitation–recrystallization interaction during annealing. For example, differential scanning calorimetry (DSC) could be performed on the MMCs tested in this study to identify temperature at which phase changes (dissolution of precipitates etc.) occur. The DSC results could be supplemented with transmission electron microscope (TEM) investigations to explain interaction between precipitates and recrystallized grains.

Acknowledgements

The authors wish to thank Mr. S. Sasidhara and Mr. M. S. M. Saifullah, Department of Metallurgy, for their assistance during the experiments and preparation of manuscript, respectively, and also the Department of Science and Technology, India, for financial support during the course of the investigation.

References

1. R. D. DOHERTY, in Proceedings of Recrystallization and Grain Growth of Multi-phase and Particle Containing Materials, Denmark, 1980, edited by N. Hansen, A. R. Jones and T. Leffers (Riso National Laboratory, Roskilde) p. 57.
2. F. J. HUMPHREYS, *ibid.* p. 35.
3. H. M. CHAN and F. J. HUMPHREYS, *Acta Metall. Mater.* **32** (1984) 527.
4. F. J. HUMPHREYS, W. S. MILLER and M. R. DJAZEB, *Mater. Sci. Tech.* **6** (1990) 1157.
5. N. HANSEN and D. JUUL JENSEN, in Proceedings of Recrystallization '90, Australia, 1990, edited by T. Chandra (*Metall. Soc. of AIME*, Warrendale, Pennsylvania) p. 79.
6. R. A. SHAHANI and T. W. CLYNE, *Mater. Sci. Tech.* **135** (1991) 281.
7. M. FERRY, P. R. MUNROE and A. CROSKY, *Scripta Metall.* **28** (1993) 1235.
8. D. YU, P. R. MUNROE, S. BANDYOPADHYAY and A. P. MOURITZ, *ibid.* **30** (1994) 927.
9. R. J. ARSENAULT and N. SHI, *Mater. Sci. Engng.* **81** (1986) 175.
10. K. K. CHAWLA and M. METZGER, *J. Mater. Sci.* **7** (1972) 34.
11. F. J. HUMPHREYS and P. N. KALU, *Acta Metall.* **38** (1990) 917.
12. F. J. HUMPHREYS, *Met. Sci.* **13** (1979) 136.
13. C. ZENER, *Trans. AIME* **47** (1948) 175.
14. T. CHANDRA and D. YU, *Mater. Forum* **15** (1991) 343.
15. M. FERRY, P. MUNROE, A. CROSKY and T. CHANDRA, *Mater. Sci. Tech.* **8** (1992) 43.
16. M. K. SURAPPA and P. K. ROHATGI, *J. Mater. Sci.* **16** (1981) 983.
17. E. E. UNDERWOOD, "Quantitative Stereology" (Addison-Wesley, MA, 1970).
18. J. E. HATCH, "Aluminium – Properties and Physical Metallurgy" (ASM, Metals Park, OH, 1984).
19. F. J. HUMPHREYS, *Mater. Sci. Engng.* **A135** (1991) 267.

Received 29 April 1994
and accepted 16 August 1995